JOURNAL OF THE ATMOSPHERIC SCIENCES

Surface Flux Feedbacks in Idealized Simulations of Tropical Depression Spinup

VARUN S. MURTHY* AND WILLIAM R. BOOS

Department of Geology and Geophysics, Yale University, New Haven, Connecticut

ABSTRACT

An idealized, three-dimensional, cloud-system resolving model is used to investigate the role of surface enthalpy flux feedbacks during tropical depression (TD) spinup, an early stage of tropical cyclogenesis in which the role of surface fluxes has not been well examined. A wide range of simulations supports the hypothesis that a negative radial gradient of surface enthalpy flux is necessary for TD spinup but can arise from multiple mechanisms. The negative radial gradient is typically created by the wind speed-dependence of surface enthalpy fluxes, consistent with previous theories for tropical cyclone intensification. However, when surface enthalpy fluxes are prescribed to be independent of wind speed, spinup still occurs, albeit more slowly, with the negative radial gradient of surface enthalpy flux maintained by an enhanced air-sea thermodynamic disequilibrium beneath the cold-core of the incipient vortex. The distinction between surface latent and sensible heat fluxes is unimportant during TD spinup; suppressing all latent heat flux while increasing the sensible heat flux to maintain roughly the same net enthalpy flux produces a rate of intensification nearly identical to that of the control. Surface enthalpy flux feedbacks seem to be more important for intensification than the vortex initial state. For example, a vortex does form and intensify even from a state of rest when the center of the domain is initialized to be nearly saturated with water vapor, but this intensification is modest in amplitude and transient, lasting less than 12 hours, without interactive surface enthaply flux.

1. Introduction

While tropical cyclogenesis was identified as the most challenging aspect of tropical cyclone research (Emanuel 2003), its understanding has been advanced by field campaigns, numerical simulations, and theory. Tropical cyclogenesis (TC genesis) refers to the series of events leading to the formation of a tropical, warm-core, cyclonic vortex. Tropical depression (TD) spinup is an early phase of TC genesis, which culminates in a region of high column relative humidity, a closed cyclonic circulation, and sustained surface wind speeds less than 17 m s^{-1}. The subsequent intensification of warm-core tropical cyclones (TCs) to hurricane strength (i.e. sustained surface wind speeds exceeding 33 m s^{-1}) has been studied extensively, but the mechanisms responsible for intensification and moistening during the earlier stage of TD spinup are less thoroughly explored.

Precipitating convection has long been associated with TC genesis (Palmen 1948). It is now widely accepted that a precipitating, thermally direct secondary circulation converges vorticity and is responsible for the system scale intensification during TC genesis (Tory and Frank 2010, references therein). As moist convection becomes stronger and more organized in a nearly saturated vortex core, the convergence of vorticity takes place at progressively lower levels and eventually leads to a TC with peak winds at the surface (Raymond and Carrillo 2011).

However, the lower troposphere of a nascent TD is often unsaturated, with moist convection there accompanied by evaporatively driven downdrafts that diverge vorticity and are hence unfavorable to TD spinup (Bergeron 1954). Downdrafts are suppressed by the increase of mid-tropospheric moist entropy within the storm, achieved through high values of column relative humidity (CRH). A negative radial gradient of CRH was deemed necessary for TC genesis in early axisymmetric studies (Emanuel 1997; Frisius 2006), and was observed in numerous field campaigns (e.g. Bister and Emanuel 1997) and high resolution numerical simulations (e.g. Wang 2012). Dunkerton et al. (2009) proposed the marsupial pouch framework, in which the critical layer of a tropical wave is most conducive for TC genesis. While the pouch initially contains more moisture than its environment, further moistening occurs during TC genesis (Wang 2012). The moistening that occurs during TD spinup, which results in a mesoscale region of nearly saturated air, is critical for some theories of subsequent TC intensification (e.g. Emanuel 1989).

*Corresponding author address: Varun S. Murthy, Department of Geology and Geophysics, Yale University, P.O. Box 208109, New Haven, CT 06520-8109.
E-mail: varun.murthy@yale.edu

A prominent theory for TC intensification involves the increase of boundary layer equivalent potential temperature by surface sensible and latent heat fluxes, and the subsequent increase of upper-tropospheric temperatures in the convecting atmosphere. In particular, a positive feedback between TC surface winds and surface enthalpy fluxes, termed wind-induced surface heat exchange (WISHE; Emanuel 1986; Rotunno and Emanuel 1987), has been examined extensively throughout the TC life cycle and found to be essential for the successful numerical simulation of at least one observed TC (Hurricane Edouard, 2014; Zhang and Emanuel 2016). In an axisymmetric model with parameterized convection, tropical cyclogenesis was attributed to a finite-amplitude instability involving the wind dependence of surface fluxes (Emanuel 1989). In a theory for TD spinup, Raymond et al. (2007) also proposed that wind-dependent surface enthalpy fluxes increase CRH, which causes an increase in the precipitating ascent that converges low-level vorticity. In contrast, Montgomery et al. (2006) argued that WISHE is not needed for TC genesis, and that intensification instead occurs because of the merger of positive vorticity anomalies generated by individual moist convective updrafts. Since Montgomery et al. (2006) initialized their numerical simulations with a moist vortex, it is unclear whether their mechanism could explain the earlier process of TD spinup wherein vortex moistening is a characteristic trait. Whether feedbacks between surface winds and surface fluxes are necessary for the intensification of weak, elevated vortices with a large saturation deficit (i.e. TD spinup) is thus an open question.[1]

Surface flux feedbacks involving the air-sea enthalpy disequilibrium have received far less attention than those involving surface winds. Yet TDs are often characterized by peak mid-level vorticity in balance with a lower tropospheric cold-core (e.g. Yanai 1961; Raymond 2012), which has been hypothesized to increase surface enthalpy fluxes because of its enhanced air-sea thermodynamic disequilibrium (Tory and Frank 2010; Davis and Ahijevych 2013). However, in a study of the spontaneous TC genesis that occurs after moist convection self-aggregates in a cloud-system resolving model, Wing et al. (2016) found that the air-sea disequilibrium provides a negative feedback on intensification. There is thus no clear agreement about the role of air-sea enthalpy disequilibrium during TD spinup.

How important is surface evaporation in moistening the TD vortex? Emanuel (1997) suggested that ocean surface evaporation moistens the atmosphere when CRH is low, with convective heating occuring only after the column is nearly saturated. In an axisymmetric model, Frisius (2006) found that surface evaporation enhanced by surface wind is required for maintaining a region with high CRH. While these studies suggest that surface evaporation increases the CRH of incipient TDs, causation is difficult to assess because surface evaporation is typically small compared to the horizontal convergence of water by the secondary circulation (e.g. Fritz and Wang 2014).

The main goal of this paper is to examine the role of surface enthalpy flux feedbacks during TD spinup, with emphasis on surface winds and air-sea enthalpy disequilibrium. Idealized cloud system resolving simulations of intensifying vortices are conducted in the absence of mean vertical wind shear, using an ensemble of initial conditions and modifications of surface fluxes. While baroclinic influences might be important for aspects of TD spinup (e.g. Davis and Bosart 2003), this study explores the idealized scenario of intensification in a barotropic base state that has been used in many prior TC studies (e.g. Rotunno and Emanuel 1987; Montgomery et al. 2009).

This study focuses on the role played by surface fluxes during TD spinup in a numerical model that explicitly represents convective-scale positive vorticity anomalies generated by cumulus updrafts – vortical hot towers (VHTs). These VHTs were proposed to be part of a non-axisymmetric pathway to TC genesis, with the positive vorticity anomalies being preferentially advected toward the center of the larger-scale vortex to merge and produce TC intensification (e.g. Hendricks et al. 2004; Montgomery et al. 2006; Tory et al. 2006). Here, the primary focus is the system scale intensification of a TD, and nearly all metrics and discussion focus on azimuthal means. Examination of horizontal distributions of instantaneous vorticity nevertheless confirms that the model simulates VHTs, validating this model as a tool for testing the hypothesis that a negative radial gradient of surface enthalpy flux is required for TD spinup.

The next section describes the numerical model and its configuration and section 3 details relevant metrics. Section 4 elucidates the role of surface flux feedbacks during spinup and section 5 quantifies the relation between intensification rates and enthalpy flux gradients. The paper concludes with a summary and discussion of the results.

2. Simulation Design

a. Model details

Simulations are performed using version 6.3 of the System for Atmospheric Modeling (SAM; Khairoutdinov and Randall 2003), a three-dimensional, Cartesian-coordinate atmospheric model that solves prognostic equations for winds, liquid water/ice moist static energy, total non-precipitating water, and total precipitating water using the anelastic approximation. We use a single moment, five

[1]The term WISHE has traditionally been used in association with a mechanism in which surface fluxes enhanced by surface winds rapidly (within a few hours) cause convective heating near the vortex center. Since deep convective heating may not occur while the core of a subsaturated TD undergoes moistening, positive feedbacks between surface winds and surface fluxes are not termed WISHE here, consistent with Raymond et al. (2007).

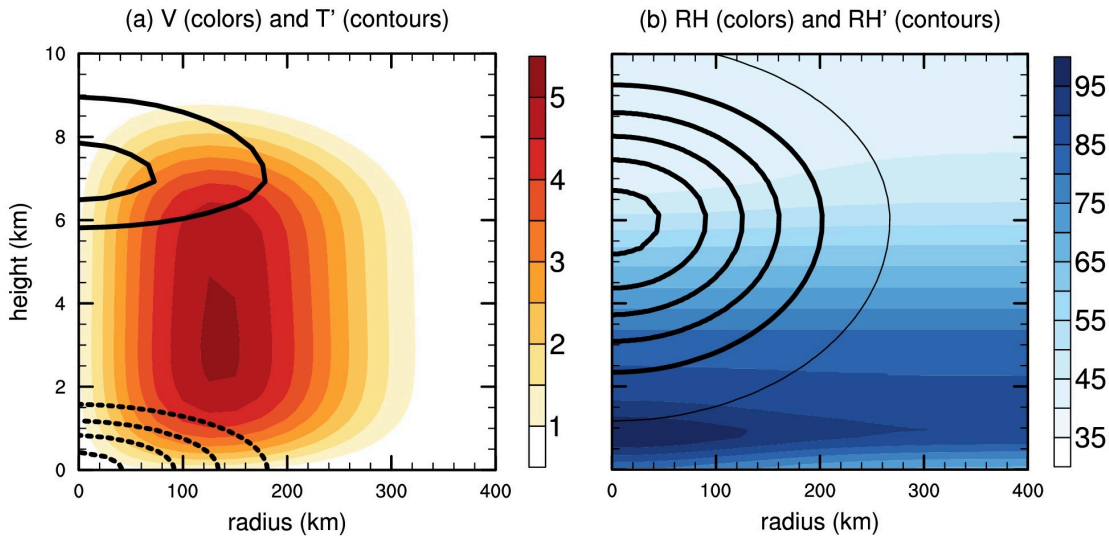

FIG. 1. (a) Axisymmetric tangential wind (colors) and axisymmetric temperature anomaly (contours, interval of 0.5 K and dashed negative) of the initial vortex in the control (Mid5, mid-level vortex with peak winds of 5 m s^{-1}) simulation. The temperature anomaly is with respect to the initial domain mean temperature. (b) Azimuthal average relative humidity (RH) of the initial state (colors) in the control (Mid5) simulation. RH of the moisture perturbation used in the group G (see Table 1) simulations is shown by contours (interval of 5%, thin contour depicts zero perturbation.)

species microphysics scheme that represents the evolution of cloud water, cloud ice, rain, graupel, and snow. A Smagorinsky-type closure is used to represent sub-grid scale turbulence. The lower boundary is an oceanic surface with fixed sea surface temperature (SST) of 301 K. The surface sensible heat flux (SHF) and latent heat flux (LHF) are parameterized using bulk formulae,

$$\begin{aligned} LHF &= \rho_0 C_E L_v U (q^*_{SST} - q_v) \\ SHF &= \rho_0 C_H c_p U (SST - T_a) \end{aligned} \tag{1}$$

where U, q_v, and T_a are, respectively, the wind speed, water vapor mixing ratio, and absolute temperature at the lowest model level, q^*_{SST} is the saturation water vapor mixing ratio at the SST and surface pressure, L_v is the latent heat of vaporization, and c_p is the specific heat of air at constant pressure. The density at the lowest model level, ρ_0, is the same value used in the anelastic equations and has no spatial or temporal variations. The bulk exchange coefficients for latent and sensible heat, C_E and C_H, respectively, are fixed at 1.1×10^{-3}. A minimum value of 1 m s^{-1} is imposed on U to crudely account for sub-grid scale variability of surface winds. The simulations are performed on an f-plane with the Coriolis parameter $f = 5 \times 10^{-5}$ s^{-1}. Parameterizations from the National Center for Atmospheric Research (NCAR) Community Climate Model (CCM3; Kiehl et al. 1998) are used to represent longwave and shortwave radiation. Insolation is fixed at a perpetual value of 409 W m^{-2}, with no diurnal or seasonal cycle.

All simulations use a 1024 × 1024 × 64 grid, with a horizontal resolution of 2 km and doubly periodic lateral boundaries. The lowest model level is at 37 m, and the vertical resolution is roughly 250 m below 2 km and 400 m in the rest of the troposphere. The upper boundary is a rigid lid at 27 km and Newtonian damping is applied in the upper third of the domain to prevent gravity wave reflection. The model uses adaptive time stepping, with a maximum time step of 5 s and automatic halving to retain numerical stability.

b. Initial conditions

All numerical simulations are initialized with horizontally homogeneous temperature and moisture profiles and no background wind. The temperature and moisture profiles are the horizontal average of the final 25 days of a 100 day simulation integrated over a smaller domain (80 × 80 × 64 grid points) with the same horizontal resolution and boundary conditions. Such initial conditions have previously been used to study tropical cyclogenesis starting from radiative-convective equilibrium (RCE; e.g. Nolan et al. 2007). The relative humidity (RH) is greater than 90% both in the lower troposphere (0 - 2 km altitude) and at the tropopause (13 - 14 km altitude), consistent with the "C" shape of the time mean tropical RH (e.g. Romps 2014). With a surface temperature of 301 K, the initial sounding has surface-based, pseudo-adiabatic convective available potential energy (CAPE) of 1200 J kg^{-1}.

TABLE 1. List of idealized simulations.

Group	*Name*	*Description*
Group A: Control simulation	Mid5	Initial vortex has peak winds of 5 m s^{-1} at an altitude of 3 km. Surface fluxes are a function of surface wind speed and air-sea enthalpy disequilibrium.
Group B: Initial condition ensemble.	Mid5_CAPEx1.5	Initial CAPE is increased by a factor of 1.5 everywhere in domain by applying a Gaussian shaped, negative temperature anomaly (peak amplitude = -3 K) to the temperature sounding between 1 km and 15 km altitude.
	Mid5_RH85	Initial RH is set to 85% from the surface to 15 km everywhere in domain.
	Sfc5	Initial vortex has peak winds of 5 m s^{-1} at the surface. The initial vertically averaged circulation of the vortex in this simulation is equal to the control.
Group C: Surface fluxes driven purely by air-sea enthalpy disequilibrium.	Mid5_Fix10	Surface wind is fixed at 10 m s^{-1} when computing surface enthalpy fluxes.
	Sfc5_Fix10	Initial vortex has peak winds of 5 m s^{-1} at the surface and surface wind is fixed at 10 m s^{-1} when computing surface enthalpy fluxes.
	Mid5_Fix5	Surface wind is fixed at 5 m s^{-1} when computing surface enthalpy fluxes.
Group D: Horizontally homogeneous surface enthalpy fluxes.	Mid5_FlxOFF	Surface enthalpy fluxes are switched off.
	Mid5_FlxHOM	Surface enthalpy fluxes are horizontally homogenized at each model time step.
	Mid5_LHF200	Surface evaporation is fixed at 200 W m^{-2}, sensible heat flux is switched off.
Group E: Horizontally homogeneous surface evaporation.	Mid5_LHF0	Surface evaporation is switched off and sensible heat flux is interactive.
	Mid5_LHF0_SHFx5	Surface evaporation is switched off and the sensible heat flux is increased by a factor of 5.
Group F: Surface winds capped in the surface enthalpy flux parameterization.	Mid5_Cap2	Surface wind is capped at 2 m s^{-1} when computing surface enthalpy fluxes.
	Mid5_Cap5	Surface wind is capped at 5 m s^{-1} when computing surface enthalpy fluxes
Group G: Simulations initialized with a moist anomaly.	Mid5_Moist	In addition to a mid-level vortex with peak winds of 5 m s^{-1}, the domain is initialized with a moist anomaly.
	Mid5_Moist_FlxOFF	Same as Mid5_Moist, but surface fluxes are switched off.
	V0_Moist	Domain is initialized only with a moist anomaly; initial tangential winds are set to 0 m s^{-1}
	V0_Moist_FlxOFF	Same as V0_Moist, but surface fluxes are switched off.
	V0_Moist_LHF200	Same as V0_Moist, but surface evaporation is fixed at 200 W m^{-2}.
Miscellaneous simulations.	Mid5_ΔTΔqHOM	Temperature and moisture disequilibria (ΔT and Δq respectively) are horizontally homogenized at each model time step prior to the computation of surface fluxes.

c. Structure of the seed vortex

A weak, balanced, axisymmetric vortex, characterized by a tangential wind field $V(r,z)$, is introduced in the center of the domain. The wind is in gradient balance with an axisymmetric temperature perturbation, $T'(r,z)$, which is tapered to zero at a radius r of 500 km (detailed equations specifying T' and V are given in the appendix). In a majority of our simulations, including the control (Mid5, see Table 1), a mid-level vortex in balance with a warm-over-cold temperature structure (Fig. 1a) is used as an idealization of TC precursors (e.g. Raymond et al. 1998). The temperature perturbation is tuned to obtain maximum winds of 5 m s^{-1} at 3 km altitude and about 150 km radius, surface wind speed that is one quarter the maximum wind speed at 3 km, and winds that taper to zero at 10 km. Some simulations are instead initialized with a vortex having peak winds at the surface, with T' positive throughout the troposphere.

The temperature anomaly associated with the axisymmetric vortex modifies the RH of the otherwise horizontally homogeneous initial state. For a mid-level vortex, this increases RH in the lower troposphere and decreases it in the upper troposphere (Fig. 1b, shading).

Additional simulations are initialized with a positive moisture anomaly in the center of the domain. The moisture anomaly is introduced as an axisymmetric RH perturbation, $RH'(r,z)$, with a maximum value of 30% at an

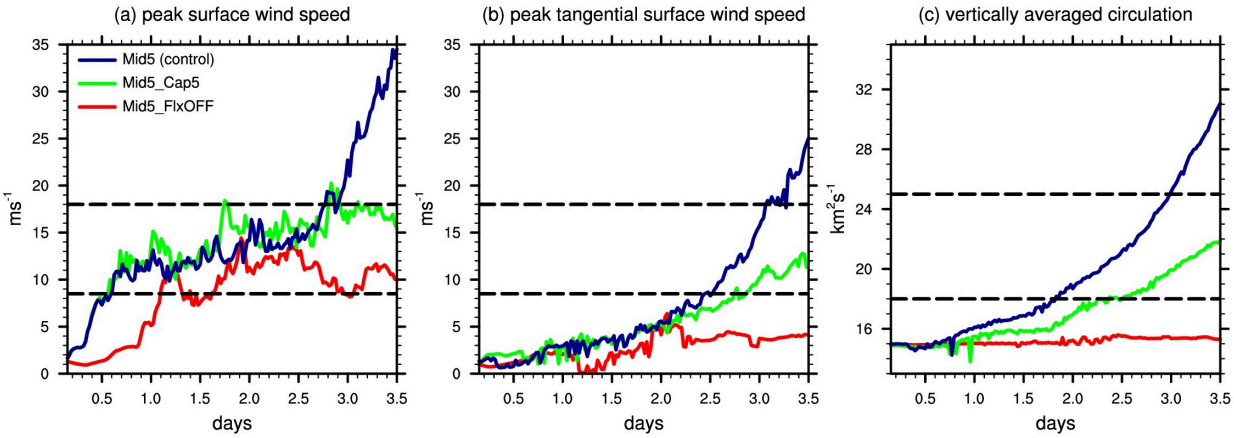

FIG. 2. Time evolution of (a) peak surface wind speed, (b) storm centered, peak azimuthal mean tangential surface wind, and (c) storm centered, 0-10 km vertically averaged circulation in the control simulation(Mid5), simulation with surface wind capped at 5 m s^{-1} in the surface flux parameterization (Mid5_Cap5) and simulation with surface fluxes switched off (Mid5_FlxOFF). The average circulation is obtained by integrating the absolute vorticity in a 500 km square around the storm center and subsequently averaging between 0-10 km. Dotted lines depict the lower and upper thresholds of wind speed and circulation used to identify tropical depressions.

altitude of 6 km (Fig. 1b, contours). The formulation of RH' is presented in the appendix.

d. List of simulations

The idealized simulations are divided into seven groups (Table 1), each designed to examine a specific aspect of surface flux feedbacks during TD spinup. The first part of the name given to each simulation indicates the altitude and intensity of the vortex. In most simulations, a mid-level vortex with peak wind speed of 5 m s^{-1} at 3 km altitude is used, indicated by the prefix "Mid5". The prefix "Sfc" indicates a vortex with peak winds at the surface, in which case the initial vertically averaged circulation is set equal to that in the control. The prefix "V0" is used when no initial vortex is used (i.e. the initial condition is a state of rest).

Subsequent parts of the names given to each simulation denote properties of the initial condition (groups B and G) or modifications to the bulk flux formulae for sensible and latent heat (groups C-F). Section 4 discusses results from these simulations, along with their design and objectives.

3. Analysis Methods

a. Metric for TD spinup

The National Oceanic and Atmospheric Administration's National Hurricane Center (NOAA-NHC) defines a TD as a cyclonic vortex with peak surface winds not exceeding 17 m s^{-1}. Since this definition lacks a lower wind speed threshold, we seek a metric that could be used to define TD spinup.

The importance of an appropriate metric is illustrated by three of our simulations: the control (Mid5), a simulation in which surface wind speeds in the surface flux parameterization are limited to 5 m s^{-1} (Mid5_Cap5), and a simulation in which surface enthalpy fluxes are eliminated entirely (Mid5_FlxOFF). Results from these simulations are discussed in detail in the next section, with select time series shown here to illustrate the importance of an appropriate spinup metric. In these simulations, inspection of the three dimensional wind field shows that the vortex in Mid5 intensifies the fastest and transitions into a warm-core vortex on day 3. In contrast, Mid5_FlxOFF exhibits no vortex intensification, and the vortex in Mid5_Cap5 intensifies more slowly than in the control and transitions into a warm-core vortex on day 4 (not shown). However, peak surface wind speeds in all three simulations are very similar from day 1.0 through day 2.5 (Fig. 2a). The threshold of 8.5 m s^{-1} marked in Fig. 2a is used by the India Meteorological Department to classify synoptic-scale vortices as monsoon depressions (Saha et al. 1981); many of the dynamical structures and genesis statistics of monsoon depressions are similar to those of TCs (Cohen and Boos 2016; Ditchek et al. 2016). All three of our vortices exceed the 8.5 m s^{-1} threshold, even though the Mid5_FlxOFF vortex does not intensify. This seems to be due to convective gustiness, showing that the peak surface wind speed is a poor measure of TD spinup.

The maximum speed of the azimuthal mean tangential surface wind enables a clearer distinction between intensifying and non-intensifying vortices (Fig. 2b). However, ambiguity about the degree of intensification persists during the first 2 to 2.5 days of the simulations.

An appropriate metric should capture changes in elevated winds to account for intensification of a mid-level vortex that might not manifest at the surface. Here, we use the circulation vertically averaged between the surface and 10 km,

$$\Gamma = \left\langle \iint (f + \nabla \times \mathbf{u})\, \mathrm{d}x\mathrm{d}y \right\rangle, \tag{2}$$

where $\mathbf{u}$ is the horizontal velocity, angle brackets denote mass-weighted vertical averages between the surface and 10 km, and the area integral is calculated over a square 500 km wide centered on the surface pressure minimum. The time evolution of this vertically averaged circulation clearly depicts differences in the intensification of the three vortices (Fig. 2c). Marín et al. (2008) used a similar metric, albeit with different horizontal and vertical extent, to depict TC intensification. Here, thresholds of 18 and 25 km^2 s^{-1}, respectively, are used to define the bounds between which a TD exists, and are determined empirically. A warm-core vortex formed in a wide range of our simulations for $\Gamma > 25$ km^2 s^{-1}, signaling the end of TD spinup. A value of $\Gamma = 18$ km^2 s^{-1} typically coincided with peak mid-level tangential winds of 8.5 m s^{-1}, average CRH values beyond 80%, and a prominent increase in precipitation rates. These thresholds vary with the horizontal extent of integration and the depth of vertical averaging.

b. Decomposition of surface fluxes

To estimate the individual contributions of surface wind speeds and air-sea thermodynamic disequilibrium to TD spinup, the total surface enthalpy flux is decomposed into wind-driven and disequilibrium-driven components. Following Wing and Emanuel (2014), we linearize Eq. (1) about the domain mean state,

$$\begin{aligned} SF' = {} & \rho_0 U' \left(C_E L_v \overline{\Delta q} + C_H c_p \overline{\Delta T}\right) \\ & + \rho_0 C_E L_v \bar{U} \Delta q' + \rho_0 C_H c_p \bar{U} \Delta T' \end{aligned} \tag{3}$$

where overbars and primes denote, respectively, horizontal domain mean quantities and corresponding spatial anomalies. The three main terms on the right hand side of Eq. (3) are the wind, moisture disequilibrium ($\Delta q = q^*_{SST} - q_v$) and temperature disequilibrium ($\Delta T = SST - T_a$) driven anomalies, respectively. Flux anomalies due to the product of anomalies of surface wind and thermodynamic disequilibrium are extremely small in our simulations. Furthermore, density anomalies do not appear in Eq. (3) due to constant density in Eq. (1), consistent with the anelastic approximation.

4. Results

a. Surface fluxes in the control simulation

We begin by diagnostically examining variations in surface enthalpy fluxes during TD spinup in the control simulation, Mid5. Since our primary interest is the role of surface flux feedbacks, we only briefly discuss the overall dynamics of spinup, noting similarities with details discussed in previous studies.

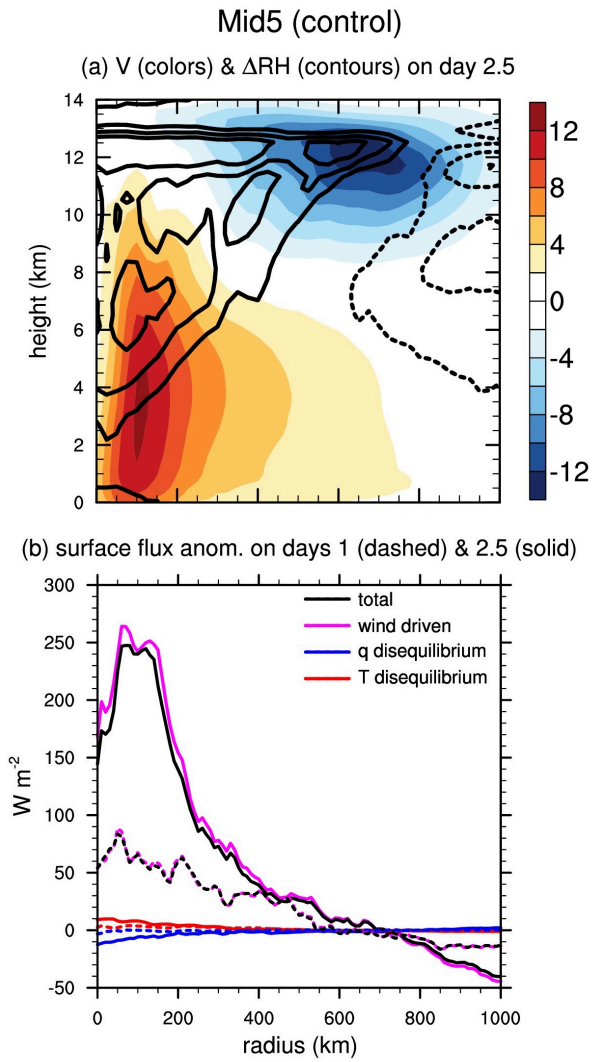

FIG. 3. (a) Azimuthal average tangential winds (colors) and increase in RH (contours, interval of 10% and dashed negative) on day 2.5 in the control (Mid5) simulation. The increase in RH is with respect to the initial moisture shown by shading in Fig. 1b. (b) Decomposition of surface flux anomalies on day 1 (dashed) and day 2.5 (solid) in the control (Mid5) simulation. The surface flux anomalies are computed with respect to the domain mean surface flux.

Intensification and moistening of the mid-level vortex, here referred to as TD spinup, last until the formation of a warm-core vortex on day 3. During the initial stages of spinup, the peak vertical mass flux occurs at approximately 7.5 km altitude (not shown). Later stages of spinup are associated with heavier precipitation rates and a lowering of the height of the peak vertical mass flux, consistent with previous observations (Raymond and Carrillo

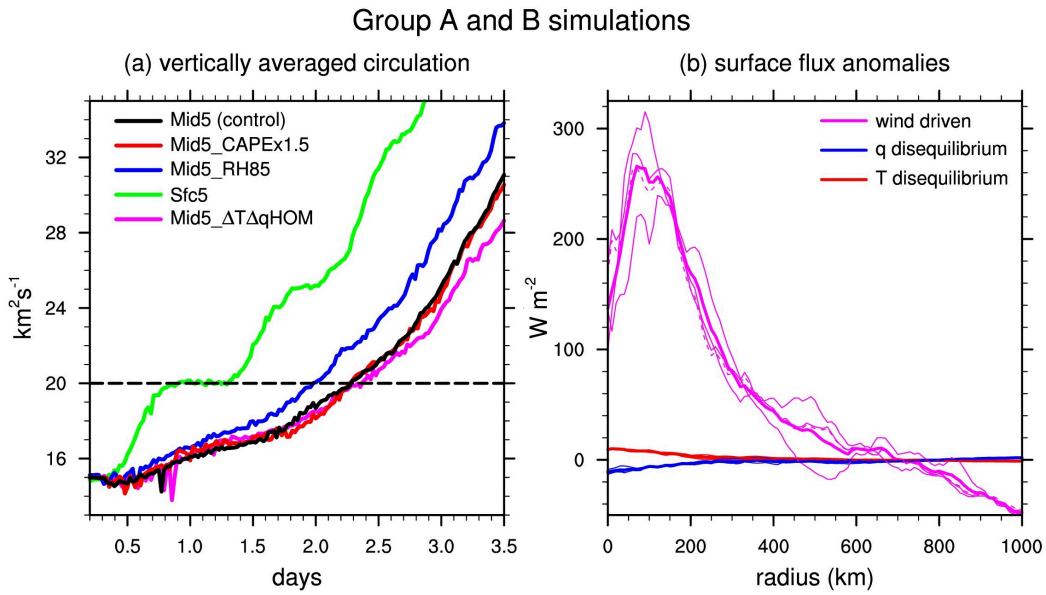

FIG. 4. (a) Time evolution of the 0-10 km vertically integrated circulation in a 500 km box tracking the vortex and (b) decomposed surface flux anomalies in the individual group B ensemble of simulations (thin solid curves) and the ensemble mean (thick solid curves). Surface flux anomalies in the ensemble members are computed when the vertically averaged circulation first reaches 20 km^2 s^{-1}, a value roughly midway through TD spinup and denoted by the horizontal dotted line in (a). The surface flux anomaly components in the control experiment are denoted by thin dashed curves in (b) and are not used to compute the ensemble mean.

2011). The vertical mass flux is associated with a radial secondary circulation hypothesized to converge vorticity. Indeed, the observed Eulerian time tendency of absolute vorticity during spinup is approximately in balance with horizontal vorticity convergence (not shown), consistent with Wang (2012).

On day 2.5, peak tangential winds occur at 3.5 km altitude and 100 km radius (Fig. 3a, shading). The mid-level vortex is associated with negative temperature anomalies (peak value $\simeq$ -3 K) below 3 km and positive anomalies (peak value $\simeq$ 2 K) above 4 km (not shown). RH increases by up to 30% compared to the initial condition, leading to values exceeding 90% (Fig. 3a, contours). High CRH has been suggested to foster large precipitation rates by reducing entrainment of dry air and suppressing downdrafts driven by evaporating precipitation (see section 1). The negative radial gradient of CRH makes the vortex, and not its environment, conducive for deep moist convection. Further details of vortex moistening are discussed in section 4e.

It has been hypothesized that the early stages of TC genesis could be strongly influenced by interactions between radiation, water vapor, and clouds (Khairoutdinov and Emanuel 2013; Wing et al. 2016). Yet in additional simulations not listed in Table 1, TD spinup occurs when radiative temperature tendencies are horizontally homogenized at each model time step, but is suppressed when the homogenization is applied to surface enthalpy fluxes. Concluding that radiative feedbacks are not essential for TD spinup in our idealized simulations, we focus purely on surface flux feedbacks, and interactions with radiation are not discussed further.

Positive surface flux anomalies occur within the vortex during TD spinup, with peak values increasing from about 80 W m^{-2} to 250 W m^{-2} between day 1 and day 2.5 (Fig. 3b, black curve). The negative radial gradient of surface fluxes is almost entirely due to wind-enhancement of surface fluxes (Fig. 3b, magenta curves). Enhanced values of near-surface water vapor mixing ratio within the vortex suppress the disequilibrium-driven surface evaporation by roughly 10 W m^{-2} on day 2.5, but the cold-core enhances disequilibrium-driven sensible heat fluxes by a similar small amount (Fig. 3b, blue and red curves). The positive and negative areas under the curves in Fig. 3b are not identical due to omission of parts of the domain (e.g. corners) during azimuthal averaging.

The influence of disequilibrium-driven surface fluxes on spinup is examined in Mid5_ΔTΔqHOM, a simulation in which the temperature and moisture disequilibria (ΔT and Δq respectively) are horizontally homogenized at each model time step prior to the computation of surface fluxes. TD spinup proceeds almost identically as in the control simulation (Fig. 4a, magenta curve), confirming the negligible role of disequilibrium-driven compared to wind-driven surface flux feedback.

b. Sensitivity to initial conditions

We now test the sensitivity of spinup in our control simulation to perturbations in initial conditions. Rather than using a large ensemble with randomly perturbed initial states, we use a three-member ensemble with large variations in initial convective available potential energy (CAPE), moisture, and initial vortex structure (Group B, Table 1). In particular, one ensemble member starts from a state in which CAPE was increased by a factor of 1.5 by applying a Gaussian shaped, negative temperature anomaly (peak amplitude = -3 K) to the initial temperature sounding between 1 km and 15 km altitude. In another ensemble member, the initial humidity was increased to achieve an RH of 85% everywhere below 15 km altitude. A third ensemble member used an initial vortex having peak winds at the surface, but the same vertically averaged circulation as the control simulation. To be clear, we do not intend to perform an exhaustive study of the sensitivity of TD spinup to initial conditions, but to provide some confirmation of the robustness of our conclusions about the role of surface flux feedbacks.

Enhanced CAPE does not accelerate TD spinup (Mid5_CAPEx1.5, Fig. 4a, red curve), presumably because moist convection consumes CAPE and restores the temperature profile to a moist adiabat faster than the roughly 3-day time scale associated with TD spinup. When initialized with 85% RH, TD spinup is accelerated (Mid5_RH85, Fig. 4a, blue curve), consistent with the hypothesis that tropospheric moistening is an important part of TD spinup. When the initial condition uses a surface vortex rather than a mid-level vortex, the rate of TD spinup increases, with rapid intensification during the first 20 hours (Sfc5, Fig. 4a, green curve). In that simulation, strong surface winds enhance surface enthalpy fluxes and lead to the convergence of vorticity by precipitating convection. After 20 hours, low-level divergence transforms the surface vortex into a mid-level vortex similar to that used in the initial condition of the control simulation.

In all members of this ensemble, enhanced surface fluxes occur near the center of the vortex during TD spinup and are driven almost entirely by surface winds (Fig. 4b). Flux anomalies driven by air-sea enthalpy disequilibrium are weak in comparison, and consist of small, counteracting latent and sensible heat flux anomalies. In summary, the rate at which TD spinup occurs is relatively insensitive to changes in CAPE and RH of the initial state, but somewhat more sensitive to the vertical structure of the seed vortex. In all cases, however, similar radial distributions of surface enthalpy fluxes occur during TD spinup and are driven almost exclusively by surface wind variations.

c. Spinup driven by air-sea enthalpy disequilibrium

While disequilibrium-driven surface fluxes played a negligible role during TD spinup in the control simulation, we now discuss a spinup mechanism driven purely by the air-sea enthalpy disequilibrium that acts when surface fluxes are independent of surface wind speed.

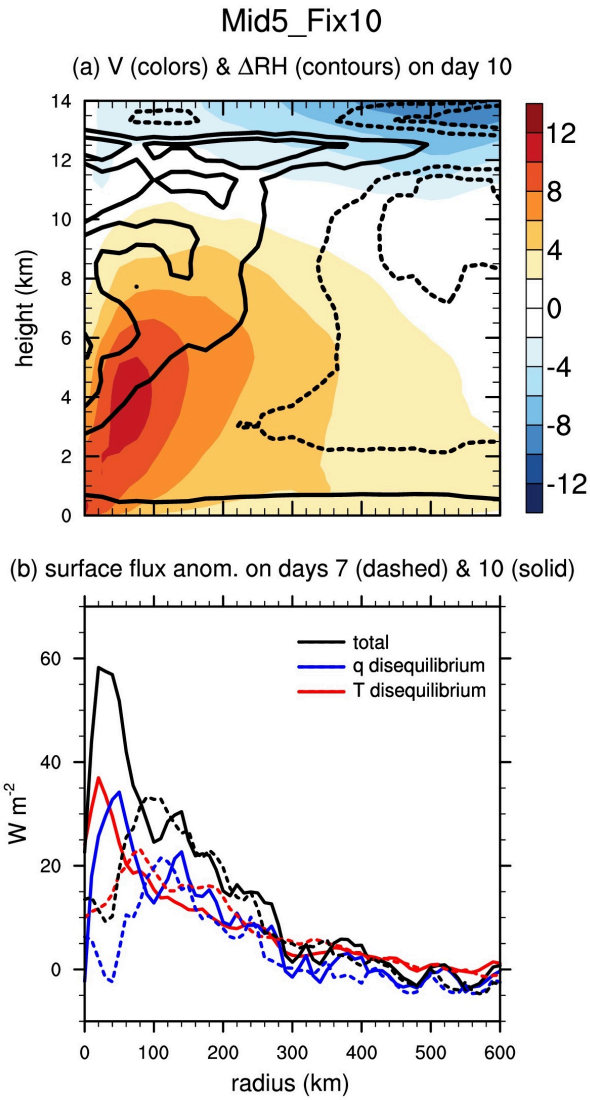

FIG. 5. Similar to Fig. 3, but for the simulation in which the surface wind is fixed at 10 m s^{-1} in the surface flux parameterization (Mid5_Fix10). Note the smaller range of the horizontal axes compared to Fig. 3. Top panel shows quantities on day 10, and bottom panel shows days 7 (dashed) and 10 (solid). Wind-driven surface flux anomalies do not exist in this simulation and are not shown in (b).

We conduct three simulations in which surface fluxes are prescribed to be independent of surface wind speed (group C, Table 1). TD spinup still occurs when the surface wind speeds are fixed at 10 m s^{-1} in the surface flux parameterization (Mid5_Fix10), albeit more slowly than in the control, with a warm-core forming on day 12 (compared to day 3 in the control; not shown). On day 10, peak winds occur at roughly 4 km altitude and at a radius of ap-

proximately 50 km (Fig. 5a). Compared to the TD in the control simulation, the vortex tilts radially outward.

Even though surface fluxes are prescribed to be independent of wind speed, spinup is still accompanied by enhanced surface fluxes near the vortex center. As in the control, the lower tropospheric negative temperature anomalies associated with the mid-level vortex enhance the sensible heat flux (Fig. 5b, red curve). Additionally, the disequilibrium-driven surface evaporation is now positive and adds to, rather than opposes, the disequilibrium-driven sensible heat flux (Fig. 5b, blue curve). The fixed wind speed of 10 m s^{-1} used in the surface flux parameterization enhances surface evaporation throughout the domain and maintains the boundary layer near saturation, depicted by a RH increase of approximately 10% below 500 m altitude at all radii (Fig. 5a). Bounded by its saturation value, the surface air water vapor mixing ratio is thus lower in the cold-core of the vortex than at large radii, leading to enhanced disequilibrium-driven surface evaporation in the vortex core. In contrast, the vortex core in the control simulation had higher specific humidity than its environment, due to the wind-enhanced surface evaporation, and so had reduced disequilibrium-driven surface evaporation in the vortex core. The existence of enhanced disequilibrium-driven evaporation thus seems to be a result of prescribing a relatively large wind speed in the surface flux formula, which brings the boundary layer near saturation and creates a positive radial gradient in the water vapor mixing ratio of surface air for a mid-level vortex. A negative radial gradient of surface enthalpy fluxes is thus obtained, driven purely by the enthalpy disequilibrium; this gradient is roughly a factor of four weaker than in the control simulation (peak surface fluxes of about 60 W m^{-2} in Mid5_Fix10 compared to 250 W m^{-2} in Mid5), consistent with the fact that it takes about four times as long for the warm-core to form (the relationship between enthalpy flux gradients and intensification rates is quantified in section 6).

When surface fluxes are independent of wind speed, the disequilibrium-driven fluxes near the vortex center seem to increase with the wind speed prescribed in the surface flux parameterization and aid spinup. That is, changes in the enthalpy of surface air do not overcompensate for the imposed changes in wind speed in Eq. (3). When the surface wind is fixed at 5 m s^{-1} in the surface flux parameterization (Mid5_Fix5), spinup proceeds more slowly than in Mid5_Fix10 and a warm-core vortex forms only on day 16 (not shown).

When initialized with a surface vortex and surface wind speeds are fixed at 10 m s^{-1} in the surface flux parameterization (Sfc5_Fix10), TD spinup is initially suppressed due to negative temperature and moisture disequilibria associated with the near-surface warm-core. Intensification occurs after low-level divergence transforms the surface vortex into a mid-level vortex. The formation of the cold-core enhances disequilibrium-driven sensible heat flux and surface evaporation during spinup, with a warm-core forming on day 14 (not shown).

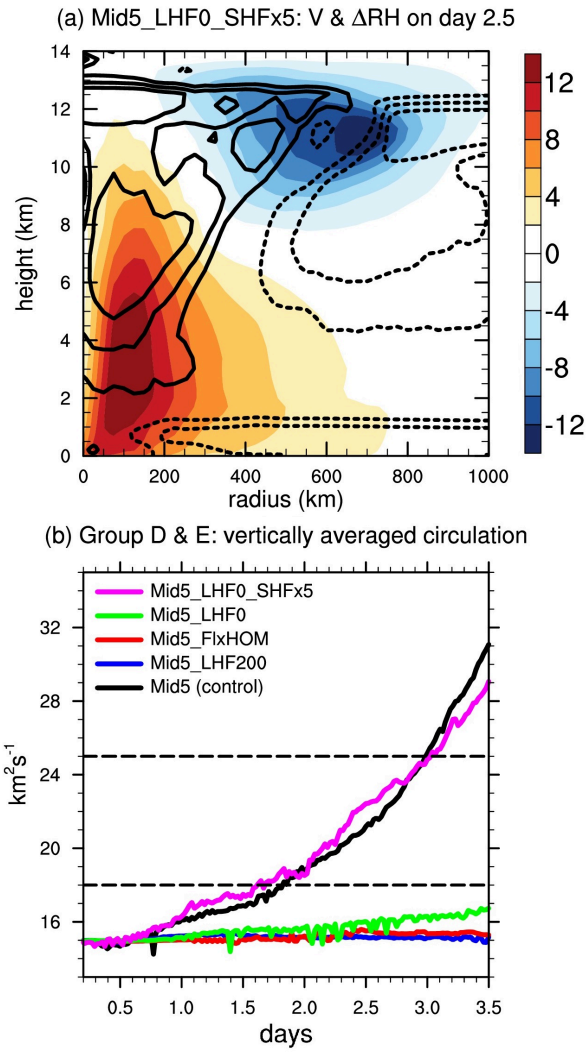

FIG. 6. (a) Same as in Fig. 3a, but for the simulation with latent heat fluxes switched off and sensible heat fluxes enhanced by a factor 5 (Mid5_LHF0_SHFx5). (b) Time evolution of the 0-10 km vertically integrated circulation in a 500 km box tracking the vortex in a few selected group D and E simulations. Dotted lines in (b) indicate the lower (18 km^2 s^{-1}) and upper (25 km^2 s^{-1}) thresholds of circulation used to identify TDs.

d. Necessity of a negative radial gradient of surface fluxes

Here, we examine whether the negative radial gradient of surface fluxes that has accompanied spinup in all prior simulations actually causes spinup by conducting a series of simulations in which horizontal inhomogeinities of surface fluxes are suppressed (group D, Table 1). As an extreme case, when surface enthalpy fluxes are entirely

switched off, TD spinup fails to occur (Mid5_FlxOFF, Fig. 2c, red curve). This result might seem to differ from one of the findings of Montgomery et al. (2006), who find that a vortex can attain TD-strength surface winds without surface enthalpy fluxes. However, mean tangential surface winds intensified to only about 12 m s^{-2} in the first 24 hours of their simulation, with no further intensification. Furthermore, Montgomery et al. (2006) initialized their model with a moister vortex, and we show in section 4g below that moister initial vortices also exhibit brief transient intensification in our model.

The necessity of surface flux feedbacks for intensification is also tested in a simulation in which the surface fluxes are fixed spatially and temporally. When surface evaporation is fixed at 200 W m^{-2} and sensible heat flux is switched off (Mid5_LHF200), the vortex fails to intensify (Fig. 6b, blue curve). Convective updrafts and downdrafts are distributed throughout the domain and the transverse secondary circulation fails to develop, despite any frictionally induced influence of the seed vortex. The fixed value of 200 W m^{-2} for latent heat flux is chosen to roughly match the peak surface fluxes in the control simulation (Fig. 3b). In additional simulations with surface enthalpy fluxes fixed at values between 50 and 350 W m^{-2}, the vortex also fails to intensify.

The failure of TD spinup to occur in the absence of a negative radial gradient of surface enthalpy fluxes is confirmed when surface enthalpy fluxes are horizontally homogenized at each model time step (Mid5_FlxHOM, Fig. 6b, red curve). These simulations support the hypothesis that surface enthalpy flux feedbacks, which manifest as a negative radial gradient of surface fluxes, are necessary for TD spinup.

e. Role of surface evaporation

The enhancement of surface enthalpy fluxes near the vortex center seems to be necessary for vortex intensification in our simulations, but how important is surface evaporation compared to surface sensible heat flux? Mrowiec et al. (2011) showed that TCs can intensify even in a dry axisymmetric model if the air-sea temperature disequilibrium is inflated to give the same net air-sea enthalpy disequilibrium as is typically observed over ocean. So, is surface evaporation needed to moisten the initial vortex so that TC intensification can then proceed in a nearly saturated atmosphere, or would an equivalent amount of sensible heat flux produce similar intensification?

Fritz and Wang (2014) showed that, for an intensifying tropical storm, horizontal convergence of water vapor by the secondary circulation closely matched total precipitation and far exceeded surface evaporation. The vertically integrated water vapor budget in our control simulation (Mid5) confirms this, with progressively larger values

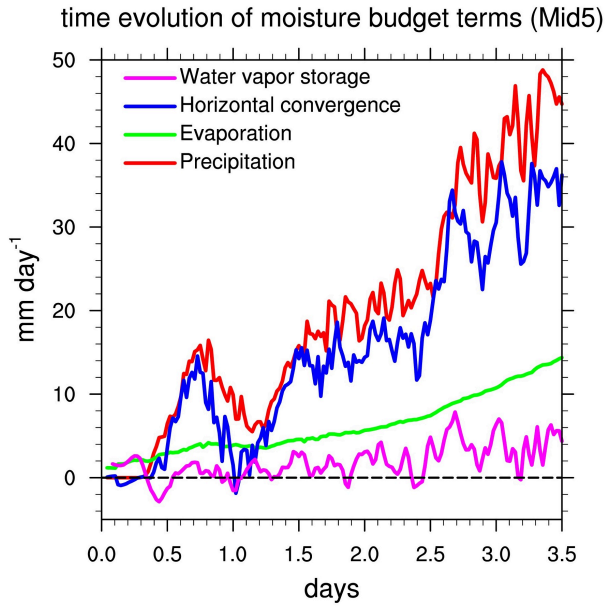

FIG. 7. Time evolution of the vertically integrated moisture budget terms in a 500 km box tracking the vortex in the control (Mid5) simulation.

of precipitation over time nearly matched by the horizontal convergence of water vapor (Fig. 7). However, surface evaporation is still larger than the storage term, even though it is small compared to horizontal convergence. Thus, based on diagnostics alone, one cannot eliminate the possibility that surface evaporation is needed to moisten the vortex and allow further intensification.

The simulations in Group E are designed to clarify the role of surface evaporation in vortex intensification and moistening. In these simulations, surface latent heat flux is switched off and replaced by a roughly equivalent amount of sensible heat flux by multiplying the exchange coefficient for sensible heat flux (C_H) by 5 (Mid5_LHF0_SHFx5). The choice of this factor is guided by the average Bowen ratio in the control simulation, 0.25, which only marginally exceeds the composite mean Bowen ratio observed in Atlantic hurricanes (0.2, Cione et al. 2000). This simulation may not have a physical analogue in the real world, but enables conclusions to be made about the role of surface evaporation in TD spinup.

In this simulation, TD spinup proceeds almost identically to the control (Fig. 6b, magenta curve). On day 2.5, mid-level cyclonic winds and RH are marginally greater than in the control simulation (Fig. 6a) and a warm-core forms on day 3. The increase in moisture is driven only by the horizontal convergence of water vapor by the transverse secondary circulation, which exceeds precipitation (not shown). Since there is no moisture source in this simulation, vortex moistening is accompanied by drying in the lower and middle troposphere outside the vortex (Fig. 6a,

dashed contours). While this does not impact the rate of TD spinup, intensification stops once the peak tangential surface wind speed reaches 56 m s^{-1} on day 7, compared to the 87 m s^{-1} attained in the control simulation on day 8 (not shown). This shows that the distinction between latent and sensible surface heat fluxes is not important in TD spinup. This essentially extends the results of Mrowiec et al. (2011), who examined the simulated structure and evolution of TCs in the total absence of water, to a moist, precipitating vortex.

We also conduct a simulation with surface evaporation switched off and interactive sensible heat fluxes, without any scaling of the transfer coefficient C_H. In this simulation (Mid5_LHF0), TD spinup is extremely slow (Fig. 6b, green curve). A warm-core vortex has not formed even after 10 days, but it is nevertheless notable that the vertically averaged circulation does increase over time. Rapid spinup over ocean in our model thus requires either interactive surface evaporation or an inflated surface sensible heat flux.

f. Surface enthalpy fluxes with "capped" wind speeds

Montgomery et al. (2009) argued that TCs do not intensify through WISHE based in part on results from simulations in which the surface wind speed in the surface flux parameterization was limited to (i.e. capped at) modest values such as 7.5 or 10 m s^{-1}. However, Zhang and Emanuel (2016) showed that the observed intensification of at least one TC (Hurricane Edouard, 2014) could only be successfully simulated if surface fluxes were not limited in that fashion. The implication of these previous results for TD spinup is unclear, because surface wind speeds during TD intensification are often below the wind speed limits imposed by Montgomery et al. (2009).

Here we also conduct simulations with wind speeds capped in the surface flux formulae but, unlike previous work, we focus on TD spinup and examine the radial distribution of surface enthalpy fluxes. Consistent with the relatively weak amplitude of TDs, we cap wind speeds in the surface flux formulae at 2 m s^{-1} and 5 m s^{-1} in two separate simulations (Group F, Table 1). Vortices in these simulations still intensify, but more slowly than in the control (Fig. 8a). There is still a clear negative radial gradient of surface enthalpy flux in both simulations, though it is also reduced in magnitude relative to that in the control (Fig. 8b; only wind-driven surface flux anomalies are plotted since the disequilibrium-driven anomalies are negligible). Even when surface winds are capped at the small value of 2 m s^{-1}, surface fluxes are enhanced by approximately 80 W m^{-2} at the radius of maximum wind compared to the vortex periphery; intensification is so slow in this case that a warm-core vortex has not formed even after 10 days, but the vertically averaged circulation does still increase over time. These results indicate that capping wind speeds in the surface flux parameterization (e.g. Montgomery et al. 2009) does not eliminate wind-evaporation feedbacks, even when wind speeds are capped at low values.

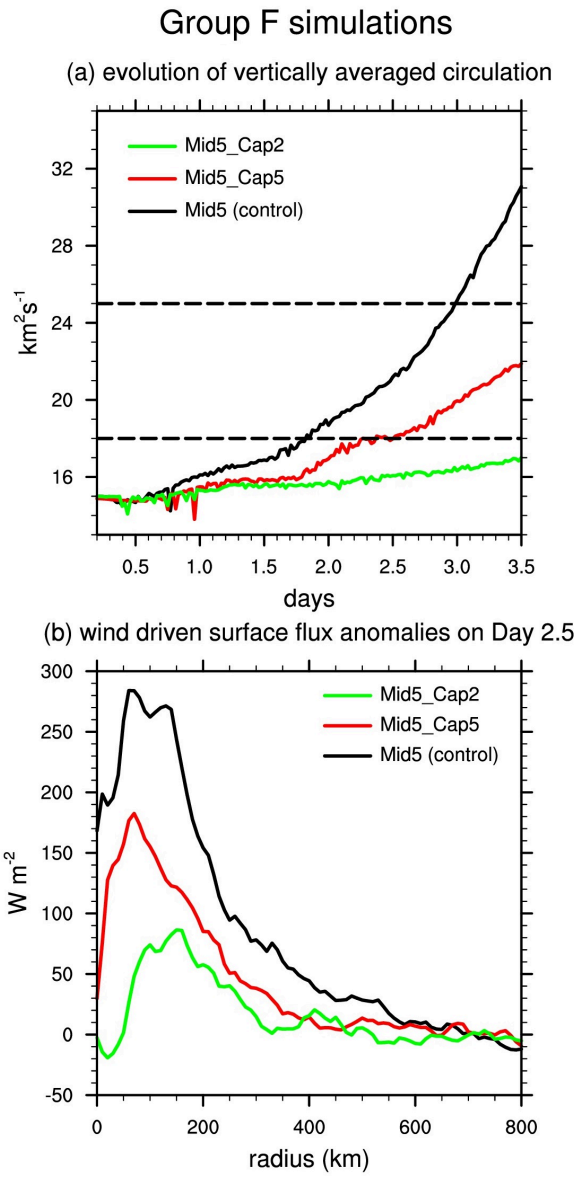

FIG. 8. (a) Evolution of the vertically averaged circulation and (b) wind driven surface flux anomalies on day 2.5 for simulations of Group F, wherein surface wind speeds are capped in the surface flux parameterization. Surface flux anomalies are calculated with respect to the domain mean. Dotted lines in (a) indicate the lower (18 km^2 s^{-1}) and upper (25 km^2 s^{-1}) thresholds of circulation used to identify TDs.

g. Transient intensification of nearly saturated vortices

Our last set of simulations examines the evolution of extremely moist initial conditions, motivated by previous studies in which a moist vortex was simulated as reaching intensities characteristic of TDs without surface flux feedbacks. In particular, Montgomery et al. (2006) stated that mean near-surface tangential winds of about 12 m s^{-1} were achieved 24 hours after initialization of their model even though surface enthalpy fluxes were turned off, but that no further intensification occurred. Does this disprove the conclusion suggested by all of our other simulations and show that surface enthalpy flux feedbacks are not needed for TD spinup?

We initialize these simulations (Group G, Table 1) by imposing a nearly saturated region (RH up to 95%) of 300 km radius in the center of the domain. The axisymmetric moisture anomaly used in these simulations is almost entirely confined to the free-troposphere (Fig. 1b, contours) and its details are given in the appendix. When this humidity field is imposed with our standard mid-level vortex as an initial condition, intensification is rapid and tropical storm intensity is attained within the first day (Mid5_Moist, Fig. 9, orange curve). This demonstrates the importance of moistening in TD spinup: much of the roughly 3 day-long spinup process in the control simulation seems to be needed primarily for tropospheric moistening, because that spinup process is shortened dramatically when a very moist initial condition is used. A nearly saturated vortex facilitates convective updrafts from the onset of the simulation and accelerates spinup. Although our initial moisture anomaly is accompanied by positive virtual temperature anomalies, those anomalies peak at 0.21 K at about 6 km altitude and are only about 20% as large as the peak warm anomalies in our mid-level and surface vortices, which intensify more slowly (e.g. compare Figs. 9 and 4a). The moist anomaly thus seems to produce faster intensification through its effect on precipitating convection rather than through its virtual temperature effect on the rotational dynamics.

More remarkable is the result that nearly identical rapid intensification can be achieved using the humidity anomaly alone without a seed vortex (i.e. by initializing the model to a state of rest with the same axisymmetric moisture anomaly just discussed). The magenta curve in Fig. 9 shows the intensification for this simulation (V0_Moist). The most rapid spinup in all of our simulations thus occurs for an axisymmetric moisture anomaly, regardless of whether an initial vortex is imposed. The rotational dynamics thus respond quite rapidly to the influence of free-tropospheric moisture on the distribution of convection, more so than they do to changes in the vertical structure of the seed vortex or even to the entire elimination of the seed vortex.

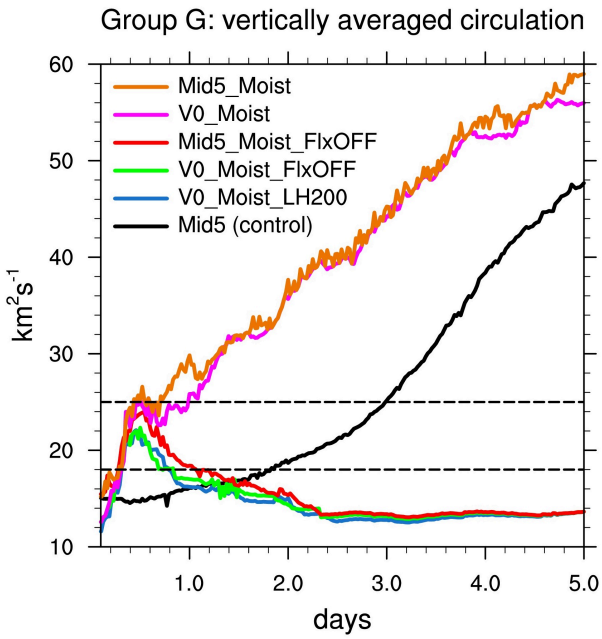

FIG. 9. Time evolution of the 0-10 km vertically integrated circulation in a 500 km box tracking the vortex in simulations initialized with an axisymmetric moist anomaly (group G). Dotted lines indicate the lower (18 km^2 s^{-1}) and upper (25 km^2 s^{-1}) thresholds of circulation used to identidy TDs. The circulation associated with the control simulation (Mid5, black curve) is plotted for reference.

A very moist seed vortex is able to undergo TD spinup when surface enthalpy fluxes are completely turned off (Mid5_Moist_FlxOFF), consistent with the result of Montgomery et al. (2006). TD spinup is rapid, with vertically averaged circulation of approximately 24 km^2 s^{-1} and peak near-surface tangential wind of 11 m s^{-1} achieved after 12 hours (Fig. 9, red curve). However, this spinup is transient and not sustained, indicated by the reduction in circulation to less than its initial value by day 3. A nearly saturated moisture anomaly at a state of rest undergoes similar transient intensification (V0_Moist_FlxOFF, Fig. 9, green curve). In this simulation, a TD-strength vortex forms within 12 hours, with peak tangential winds of 13 m s^{-1} at roughly 4 km altitude confined to radii where RH exceeds 90% (Fig. 10a). However, in the absence of surface fluxes, a warm-core vortex fails to form and the vortex and its associated moisture dissipate rapidly. After 5 days, only a weak vortex with peak wind speeds of 6 m s^{-1} and no associated moisture remains (Fig. 10b). Similar transient intensification is seen when a moist anomaly is allowed to evolve from rest with surface evaporation fixed at a horizontally uniform value of 200 W m^{-2} (V0_Moist_LH200, Fig. 9, blue curve). This confirms that, even for a very moist initial vortex, it is not the amplitude of the domain-mean surface enthalpy flux that

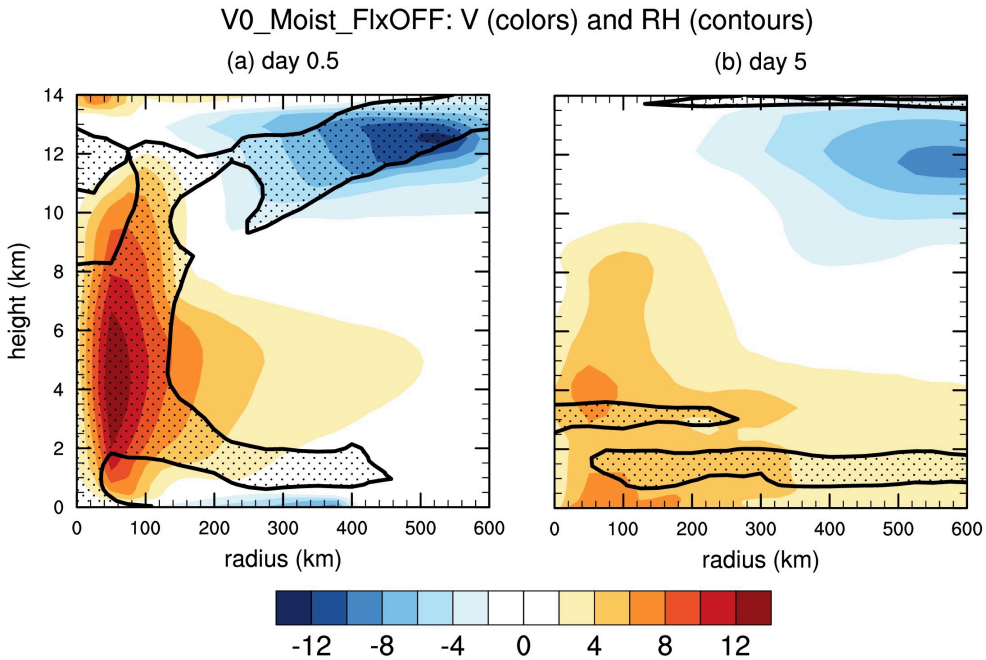

FIG. 10. Azimuthal average tangential winds (colors) and RH (contours; stippling indicates RH greater than 90%) on (a) day 0.5 and (b) day 5 in the simulation initialized with no tangential winds, an axisymmetric moist anomaly and surface fluxes switched off (V0_Moist_FlxOFF).

matters, but the enthalpy flux feedbacks with the vortex state.

5. Comparison with a theory for TD spinup

The role of enhanced surface flux in TD spinup is quantitatively assessed across all of our simulations by comparison with the theory of Raymond et al. (2007, hereafter R07), which relates the rate of change of the vertically averaged circulation, Γ, to surface fluxes of enthalpy and momentum in a nascent TD. In particular, the vorticity equation is integrated horizontally and averaged vertically over the same domain used in Eq. (2),

$$\frac{\partial \Gamma}{\partial t} = -\iint \langle \nabla \cdot (\mathbf{u}\zeta_a) \rangle \, \mathrm{d}x\mathrm{d}y - \iint \langle \nabla \cdot (\mathbf{k} \times \mathbf{F}) \rangle \, \mathrm{d}x\mathrm{d}y, \tag{4}$$

where ζ_a is absolute vorticity and $\mathbf{F}$ represents horizontal viscous and turbulent forces. Like R07, we omit the "tilting" term, $\omega\partial_p\mathbf{u}$, by neglecting the vertical velocity ω on the periphery of the area of integration. Following Neelin and Held (1987), we define a gross moist stability (GMS),

$$\gamma \equiv \frac{SF - R}{[\nabla \cdot \mathbf{u}]_+}, \tag{5}$$

with R the column-integrated radiative flux divergence and $[\nabla \cdot \mathbf{u}]_+$ the vertical integral of the positive part of the divergence profile. For simplicity, we deviate from R07 here and do not normalize the GMS by the moisture flux convergence nor weight our vertical average of the vorticity equation by the mixing ratio.

For a weak vortex in an environment of negligible horizontal shear, $\nabla \cdot (\mathbf{u}\zeta_a) \simeq f\nabla \cdot \mathbf{u}$. If the modification of R by the vortex is also neglected and SF' is the surface enthalpy flux anomaly relative to SF in radiative-convective equilibrium, then Eq. (4) becomes

$$\frac{\partial \Gamma}{\partial t} = \frac{1}{\gamma}\left(\frac{f}{M}\iint SF' \mathrm{d}x\mathrm{d}y\right) + \frac{1}{M}\iint \nabla \cdot (\mathbf{k} \times \mathbf{T}) \mathrm{d}x\mathrm{d}y, \tag{6}$$

where $\mathbf{T}$, the surface drag, is the mass-weighted vertical integral of the frictional force $\mathbf{F}$, and M is the vertically integrated mass of the initial sounding. The first term represents the spinup tendency due to vorticity convergence by the large-scale ascent needed to export the column energy input by anomalous surface fluxes. The second term represents the damping effects of drag and is equal to the line integral of surface drag on the periphery of our domain, which under a bulk flux formula is $-4a\rho_0 C_D U^2/M$ for a square domain of width a and drag coefficient C_D. Using Eq. (1) to represent SF' with $C_E = C_H = C_D$, we can estimate the relative magnitude of the spinup and spindown tendencies (i.e. the ratio of the first and the second terms) as

$$\frac{af\Delta k}{4\gamma U}, \tag{7}$$

with Δk the air-sea enthalpy disequilibrium. For $U = 10$ m s^{-1} and $\Delta k = 20$ kJ kg^{-1}, this ratio is between 25 and 2.5 for values of γ between 500 J kg^{-1} (e.g. Yu et al. 1998) and 5000 J kg^{-1} (e.g. R07, their normalized GMS of 0.5 is converted using a moisture stratification of 5 g kg^{-1}). In any case, the spindown tendency given by the line integral of the drag is smaller than that estimated by R07 for TDs with radii less than 500 km. The above treatment assumes drag to be distributed over the full depth of the vortex, perhaps by convective momentum transports and the continual readjustment of the vortex toward gradient wind balance, whereas R07 assumed drag confined to the surface layer but discussed the possibility that it might have a larger vertical length scale. In our control simulation and in Sfc5 (the initial vortex expected to exhibit the strongest drag), the spindown tendency in Eq. (6) due to surface friction is about one-fifteenth the circulation tendency when it is calculated to apply between the surface and 10 km. This may explain why our seed vortices intensify even though they have radii well below the critical radius of 1600 km predicted by R07 to be necessary for intensification.

Since the spindown term due to drag seems to be small, we compare $\partial_t \Gamma$ and the spinup term in each of our simulations, with each term averaged between the start of the simulation and the time at which Γ reaches 25 km^2 s^{-1} (in simulations without spinup, averages are computed up to day 5). The intensification rate is well correlated with the spinup term (Fig. 11), supporting the theory in which surface flux feedbacks cause TD spinup. The reciprocal of the slope of the best fit line suggests a typical GMS value of roughly 3925 J kg^{-1} across our simulations.

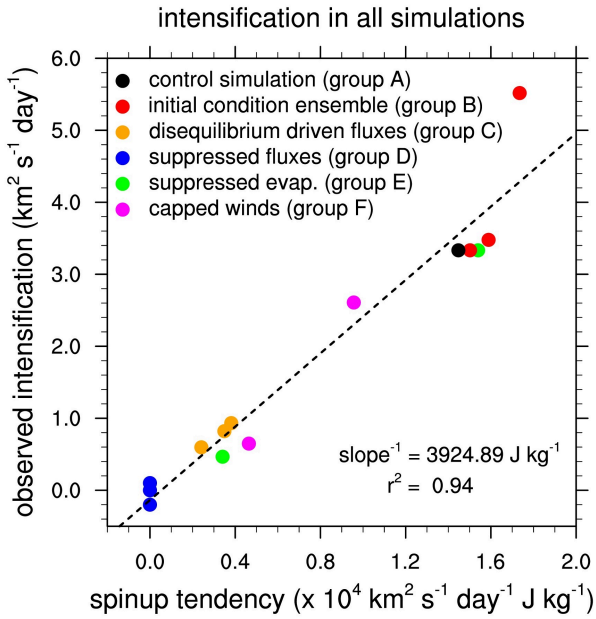

FIG. 11. Time tendency of vertically averaged circulation on the y-axis compared with the term inside the parantheses in the spinup tendency in Eq. (6) on the x-axis in all our simulations (except group G).

6. Summary and discussion

Surface flux feedbacks during TD spinup were examined here using idealized, three-dimensional, cloud-system resolving simulations of intensifying vortices over uniform SST. All simulations support the hypothesis that a negative radial gradient of surface enthalpy flux, with enhanced surface flux near the vortex center, is required for TD spinup. By decomposing the surface flux into wind- and enthalpy disequilibrium-driven components, we show that TD spinup occurs most rapidly when surface enthalpy flux is enhanced by surface winds, with the disequilibrium-driven feedback being comparatively weak. TD spinup occurs and is accompanied by a negative radial gradient of surface enthalpy flux even when surface fluxes are prescribed to be independent of surface winds, due to a negative radial gradient of air-sea enthalpy disequilibrium. In this case, however, TD spinup occurs slowly and at a rate dependent on the uniform wind speed imposed in the surface flux parameterization. Spinup fails to occur in the absence of surface enthalpy flux feedbacks and slows down when the feedbacks are reduced by limiting (i.e. capping) the wind speed in the surface flux formulae.

Additionally, when surface evaporation is replaced by a roughly equivalent amount of sensible heat flux, vortex intensification and moistening is nearly identical to the control simulation. This result, which shows that the distinction between latent and sensible heat fluxes is unimportant during spinup, is surprising since surface evaporation over oceans has traditionally been assigned an extremely important role during the spinup of tropical cyclonic vortices. Lower-tropospheric moistening by surface evaporation may thus be one way in which the vortex moist entropy is increased during TD spinup, but it is not the only way. This may have implications for the observed spinup of TDs over dry coastal land regions, where surface evaporation is limited but where abundant moisture could be fluxed from nearby oceans.

From a thermodynamic perspective, intensification and moistening of a TD is associated with an increase in its moist entropy, which can be achieved via multiple pathways: import by the secondary circulation, enhanced surface enthalpy fluxes, or reduced radiative cooling. The slope of the best-fit line in Fig. 11 suggests a positive GMS and thus an export of moist entropy by the secondary circulation. We also found (although it was not a main focus) that spinup still occurred when radiative temperature tendencies were horizontally homogenized at each model time step, which contradicts the hypothesis that reduced

radiative cooling is needed to produce the moist entropy increase that occurs during spinup. This leaves surface enthalpy fluxes as the remaining process by which the moist entropy could be increased and, indeed, TD spinup failed to occur in the absence of enhanced surface enthalpy fluxes in our simulations. Nevertheless, our analyses did not focus on the transport of moist entropy by the secondary circulation or on the role of interactions between radiation, water vapor and clouds; further investigation of these processes during TD spinup is thus needed.

Finally, we showed that a moist vortex undergoes TD spinup in the absence of surface flux feedbacks, but only in a transient, brief, and unsustained manner, lasting less than 24 hours. Surface flux feedbacks continued to be necessary for sustained intensification of a moist vortex and subsequent transition to a warm-core vortex.

The negative radial gradient of surface fluxes required for TD spinup was generated by two primary mechanisms in the idealized simulations used in this study. In a quiescent environment (e.g. simulations in Group A and B in Table 1), surface fluxes were enhanced by surface winds. Alternatively, when sufficiently strong uniform surface winds were imposed in the bulk flux formulae, which might be taken to represent a gusty environment, the air-sea thermodynamic disequilibrium enhanced the surface fluxes and led to spinup, albeit more slowly. Whether some part of the spinup process in observed TDs might be caused by air-sea thermodynamic disequilibrium is unclear, but further investigation seems merited given that typical trade wind speeds of roughly 5 m s $^{-1}$ are comparable to azimuthal surface wind speeds in the initial stages of spinup. Further investigation of the role of surface flux feedback mechanisms in more realistic background states, e.g. with vertical and horizontal shear, would help in understanding such issues.

Acknowledgments. This work was supported by Office of Naval Research awards N00014-11-1-0617 and N00014-15-1-2531 and by the Yale Center for Research Computing.

APPENDIX

Initialization of the seed vortex and moisture anomaly

a. Seed vortex

Here, we describe the structure of the seed vortex in our simulations. The temperature perturbation is considered first, followed by the balance used to compute tangential winds.

The axisymmetric temperature perturbation, $T'(r,z)$, is the product of separate vertical (T'_z) and radial (T'_r) structures. The vertical structure is governed by the maximum negative anomaly (T'_{-ve} = -2.5 K), the maximum positive anomaly (T'_{+ve} = 1.05 K), the height of maximum winds (z_m = 3 km), and the vertical extent of the vortex (z_t = 11 km),

$$T'_z(z) = \left\{ \begin{array}{ll} T'_{-ve} \times \exp\left(-\frac{z^2}{z_m^2/8}\right), & \text{for } z \le z_m \\ T'_{+ve} \times \exp\left(-\frac{(z-z_{mid})^2}{(z_t-z_m)^2/32}\right), & \text{for } z > z_m \end{array} \right\} \tag{A1}$$

where $z_{mid} = (z_m + z_t)/2$. The radial structure is governed by the radius at which the tangential winds vanish (r_{end} = 500 km),

$$T'_r(r) = exp\left(-\frac{r^2}{r_{end}^2/8}\right). \tag{A2}$$

The resulting temperature anomaly for the control simulation is shown in Fig. 1a (contours).

The axisymmetric pressure (p) and density (ρ) are computed using the hydrostatic approximation and ideal gas law,

$$\begin{gathered} \frac{\partial p}{\partial z} = -\rho g, \\ \rho = \frac{p}{R_d T(1+0.61q)}, \end{gathered} \tag{A3}$$

where T is the total temperature (including the anomaly T'), q is the water vapor mixing ratio from the sounding, R_d is the gas constant for dry air (287 J kg^{-1} K^{-1}) and g is the gravitational acceleration. The hydrostatic equation is integrated from the top of the model to the surface, with ρ calculated using the ideal gas law at each height. Pressure and density at the top level are obtained from the initial sounding.

Gradient wind balance in cylindrical coordinates is

$$\frac{v^2}{r} + fv = \frac{1}{\rho}\frac{\partial p}{\partial r} \tag{A4}$$

with v the tangential wind. The balanced tangential wind at each height is obtained from the vertical derivative of gradient wind balance,

$$\frac{\partial v}{\partial z} = -\frac{1}{\rho}\frac{\frac{1}{\rho}\frac{\partial p}{\partial r}\frac{\partial \rho}{\partial z} + g\frac{\partial \rho}{\partial r}}{(\frac{2v}{r}+f)}. \tag{A5}$$

This equation (A5) is integrated downward from $v = 0$ at the top of the model to obtain the axisymmetric tangential winds as a function of r and z. Centered finite difference schemes are used to compute the radial and vertical derivatives in Eqn. A5, except at the boundaries where appropriate forward or backward difference schemes are used. Tangential winds in the control simulation are plotted in Fig. 1a (colors).

b. Moisture anomaly

The axisymmetric, positive RH anomaly introduced into the center of the domain in a few simulations (Table 1, group G) is the product of separate vertical (RH'_z)

and radial (RH'_r) functions. The vertical structure is specified in terms of its maximum value (RH'_{max} = 30%) and its bottom (z_b = 1 km) and top (z_t = 11 km) boundaries,

$$RH'_z(z) = RH'_{max} \times \exp\left(-\frac{(z - z_{mid})^2}{(z_t - z_b)^2/32}\right) \qquad \text{(A6)}$$

where $z_{mid} = (z_b + z_t)/2$. The RH anomaly peaks at the center of the domain and vanishes at radius r_{end} = 300 km with a radial distribution

$$RH'_r(r) = exp\left(-\frac{r^2}{r_{end}^2/8}\right). \qquad \text{(A7)}$$

The RH anomaly is shown in Fig. 1b (contours). The total RH is not allowed to exceed a maximum value of 95%.

References

Bergeron, T., 1954: REVIEW OF MODERN METEOROLOGY—12. the problem of tropical hurricanes. *Q.J Royal Met. Soc.*, **80 (344)**, 131–164, doi:10.1002/qj.49708034402, URL http://dx.doi.org/10.1002/qj.49708034402.

Bister, M., and K. A. Emanuel, 1997: The genesis of hurricane guillermo: TEXMEX analyses and a modeling study. *Mon. Wea. Rev.*, **125 (10)**, 2662–2682, doi:10.1175/1520-0493(1997)125⟨2662:tgohgt⟩2.0.co;2, URL http://dx.doi.org/10.1175/1520-0493(1997)125⟨2662:tgohgt⟩2.0.co;2.

Cione, J. J., P. G. Black, and S. H. Houston, 2000: Surface observations in the hurricane environment. *Mon. Wea. Rev.*, **128 (5)**, 1550–1561, doi:10.1175/1520-0493(2000)128⟨1550:soithe⟩2.0.co;2, URL http://dx.doi.org/10.1175/1520-0493(2000)128⟨1550:soithe⟩2.0.co;2.

Cohen, N. Y., and W. R. Boos, 2016: Perspectives on moist baroclinic instability: Implications for the growth of monsoon depressions. *J. Atmos. Sci.*, **73 (4)**, 1767–1788, doi:10.1175/jas-d-15-0254.1, URL http://dx.doi.org/10.1175/jas-d-15-0254.1.

Davis, C. A., and D. A. Ahijevych, 2013: Thermodynamic environments of deep convection in atlantic tropical disturbances. *J. Atmos. Sci.*, **70 (7)**, 1912–1928, doi:10.1175/jas-d-12-0278.1, URL http://dx.doi.org/10.1175/jas-d-12-0278.1.

Davis, C. A., and L. F. Bosart, 2003: Baroclinically induced tropical cyclogenesis. *Monthly Weather Review*, **131 (11)**, 2730–2747, doi:10.1175/1520-0493(2003)131⟨2730:bitc⟩2.0.co;2, URL https://doi.org/10.1175%2F1520-0493%282003%29131%3C2730%3Abitc%3E2.0.co%3B2.

Ditchek, S. D., W. R. Boos, S. J. Camargo, and M. K. Tippett, 2016: A genesis index for monsoon disturbances. *Journal of Climate*, **29 (14)**, 5189–5203, doi:10.1175/jcli-d-15-0704.1, URL https://doi.org/10.1175%2Fjcli-d-15-0704.1.

Dunkerton, T. J., M. T. Montgomery, and Z. Wang, 2009: Tropical cyclogenesis in a tropical wave critical layer: easterly waves. *Atmospheric Chemistry and Physics*, **9 (15)**, 5587–5646, doi:10.5194/acp-9-5587-2009, URL http://dx.doi.org/10.5194/acp-9-5587-2009.

Emanuel, K., 2003: TROPICALCYCLONES. *Annu. Rev. Earth Planet. Sci.*, **31 (1)**, 75–104, doi:10.1146/annurev.earth.31.100901.141259, URL http://dx.doi.org/10.1146/annurev.earth.31.100901.141259.

Emanuel, K. A., 1986: An air-sea interaction theory for tropical cyclones. part i: Steady-state maintenance. *J. Atmos. Sci.*, **43 (6)**, 585–605, doi:10.1175/1520-0469(1986)043⟨0585:aasitf⟩2.0.co;2, URL http://dx.doi.org/10.1175/1520-0469(1986)043⟨0585:aasitf⟩2.0.co;2.

Emanuel, K. A., 1989: The finite-amplitude nature of tropical cyclogenesis. *Journal of the Atmospheric Sciences*, **46 (22)**, 3431–3456, doi:10.1175/1520-0469(1989)046⟨3431:tfanot⟩2.0.co;2, URL https://doi.org/10.1175%2F1520-0469%281989%29046%3C3431%3Atfanot%3E2.0.co%3B2.

Emanuel, K. A., 1997: Some aspects of hurricane inner-core dynamics and energetics. *J. Atmos. Sci.*, **54 (8)**, 1014–1026, doi:10.1175/1520-0469(1997)054⟨1014:saohic⟩2.0.co;2, URL http://dx.doi.org/10.1175/1520-0469(1997)054⟨1014:saohic⟩2.0.co;2.

Frisius, T., 2006: Surface-flux-induced tropical cyclogenesis within an axisymmetric atmospheric balanced model. *Quarterly Journal of the Royal Meteorological Society*, **132 (621)**, 2603–2623, doi:10.1256/qj.06.03, URL http://dx.doi.org/10.1256/qj.06.03.

Fritz, C., and Z. Wang, 2014: Water vapor budget in a developing tropical cyclone and its implication for tropical cyclone formation. *J. Atmos. Sci.*, **71 (11)**, 4321–4332, doi:10.1175/jas-d-13-0378.1, URL http://dx.doi.org/10.1175/jas-d-13-0378.1.

Hendricks, E. A., M. T. Montgomery, and C. A. Davis, 2004: The role of "vortical" hot towers in the formation of tropical cyclone diana (1984). *Journal of the Atmospheric Sciences*, **61 (11)**, 1209–1232, doi:10.1175/1520-0469(2004)061⟨1209:trovht⟩2.0.co;2, URL https://doi.org/10.1175%2F1520-0469%282004%29061%3C1209%3Atrovht%3E2.0.co%3B2.

Khairoutdinov, M., and K. Emanuel, 2013: Rotating radiative-convective equilibrium simulated by a cloud-resolving model. *Journal of Advances in Modeling Earth Systems*, **5 (4)**, 816–825, doi:10.1002/2013ms000253, URL https://doi.org/10.1002%2F2013ms000253.

Khairoutdinov, M. F., and D. A. Randall, 2003: Cloud resolving modeling of the ARM summer 1997 IOP: Model formulation, results, uncertainties, and sensitivities. *J. Atmos. Sci.*, **60 (4)**, 607–625, doi:10.1175/1520-0469(2003)060⟨0607:crmota⟩2.0.co;2, URL http://dx.doi.org/10.1175/1520-0469(2003)060⟨0607:CRMOTA⟩2.0.CO;2.

Kiehl, J. T., J. J. Hack, G. B. Bonan, B. A. Boville, D. L. Williamson, and P. J. Rasch, 1998: The national center for atmospheric research community climate model: CCM3. *Journal of Climate*, **11 (6)**, 1131–1149, doi:10.1175/1520-0442(1998)011⟨1131:tncfar⟩2.0.co;2, URL http://dx.doi.org/10.1175/1520-0442(1998)011⟨1131:TNCFAR⟩2.0.CO;2.

Marín, J. C., D. J. Raymond, and G. B. Raga, 2008: Intensification of tropical cyclones in the GFS model. *Atmospheric Chemistry and Physics Discussions*, **8 (5)**, 17 803–17 839, doi:10.5194/acpd-8-17803-2008, URL http://dx.doi.org/10.5194/acpd-8-17803-2008.

Montgomery, M. T., M. E. Nicholls, T. A. Cram, and A. B. Saunders, 2006: A vortical hot tower route to tropical cyclogenesis. *J. Atmos. Sci.*, **63 (1)**, 355–386, doi:10.1175/jas3604.1, URL http://dx.doi.org/10.1175/jas3604.1.

Montgomery, M. T., N. V. Sang, R. K. Smith, and J. Persing, 2009: Do tropical cyclones intensify by WISHE? *Quarterly Journal of the Royal Meteorological Society*, **135 (644)**, 1697–1714, doi:10.1002/qj.459, URL http://dx.doi.org/10.1002/qj.459.

Mrowiec, A. A., S. T. Garner, and O. M. Pauluis, 2011: Axisymmetric hurricane in a dry atmosphere: Theoretical framework and numerical experiments. *Journal of the Atmospheric Sciences*, **68 (8)**, 1607–1619, doi:10.1175/2011jas3639.1, URL https://doi.org/10.1175%2F2011jas3639.1.

Neelin, J. D., and I. M. Held, 1987: Modeling tropical convergence based on the moist static energy budget. *Monthly Weather Review*, **115 (1)**, 3–12, doi:10.1175/1520-0493(1987)115⟨0003:mtcbot⟩2.0.co;2, URL https://doi.org/10.1175%2F1520-0493%281987%29115%3C0003%3Amtcbot%3E2.0.co%3B2.

Nolan, D. S., E. D. Rappin, and K. A. Emanuel, 2007: Tropical cyclogenesis sensitivity to environmental parameters in radiative-convective equilibrium. *Quarterly Journal of the Royal Meteorological Society*, **133 (629)**, 2085–2107, doi:10.1002/qj.170, URL http://dx.doi.org/10.1002/qj.170.

Palmen, E., 1948: On the formation and structure of tropical hurricanes. *Geophysica*, **3 (1)**, 26–38.

Raymond, D. J., 2012: Balanced thermal structure of an intensifying tropical cyclone. *Tellus A*, **64 (0)**, doi:10.3402/tellusa.v64i0.19181, URL https://doi.org/10.3402%2Ftellusa.v64i0.19181.

Raymond, D. J., and C. L. Carrillo, 2011: The vorticity budget of developing typhoon nuri (2008). *Atmospheric Chemistry and Physics*, **11 (1)**, 147–163, doi:10.5194/acp-11-147-2011, URL http://dx.doi.org/10.5194/acp-11-147-2011.

Raymond, D. J., C. López-Carrillo, and L. L. Cavazos, 1998: Case-studies of developing east pacific easterly waves. *Quarterly Journal of the Royal Meteorological Society*, **124 (550)**, 2005–2034, doi:10.1256/smsqj.55010, URL http://dx.doi.org/10.1256/smsqj.55010.

Raymond, D. J., S. L. Sessions, and Ž. Fuchs, 2007: A theory for the spinup of tropical depressions. *Quarterly Journal of the Royal Meteorological Society*, doi:10.1002/qj.125, URL http://dx.doi.org/10.1002/qj.125.

Romps, D. M., 2014: An analytical model for tropical relative humidity. *Journal of Climate*, **27 (19)**, 7432–7449, doi:10.1175/jcli-d-14-00255.1, URL http://dx.doi.org/10.1175/jcli-d-14-00255.1.

Rotunno, R., and K. A. Emanuel, 1987: An air–sea interaction theory for tropical cyclones. part II: Evolutionary study using a nonhydrostatic axisymmetric numerical model. *J. Atmos. Sci.*, **44 (3)**, 542–561, doi:10.1175/1520-0469(1987)044⟨0542:aaitft⟩2.0.co;2, URL http://dx.doi.org/10.1175/1520-0469(1987)044⟨0542:aaitft⟩2.0.co;2.

Saha, K., F. Sanders, and J. Shukla, 1981: Westward propagating predecessors of monsoon depressions. *Monthly Weather Review*, **109 (2)**, 330–343, doi:10.1175/1520-0493(1981)109⟨0330:wppomd⟩2.0.co;2, URL https://doi.org/10.1175%2F1520-0493%281981%29109%3C0330%3Awppomd%3E2.0.co%3B2.

Tory, K. J., and W. M. Frank, 2010: Tropical cyclone formation. *From Science to Mitigation*, World Scientific Pub Co Pte Lt, 55–91, doi:10.1142/9789814293488_0002, URL http://dx.doi.org/10.1142/9789814293488_0002.

Tory, K. J., M. T. Montgomery, and N. E. Davidson, 2006: Prediction and diagnosis of tropical cyclone formation in an NWP system. part i: The critical role of vortex enhancement in deep convection. *J. Atmos. Sci.*, **63 (12)**, 3077–3090, doi:10.1175/jas3764.1, URL http://dx.doi.org/10.1175/jas3764.1.

Wang, Z., 2012: Thermodynamic aspects of tropical cyclone formation. *J. Atmos. Sci.*, **69 (8)**, 2433–2451, doi:10.1175/jas-d-11-0298.1, URL http://dx.doi.org/10.1175/jas-d-11-0298.1.

Wing, A. A., S. J. Camargo, and A. H. Sobel, 2016: Role of radiative–convective feedbacks in spontaneous tropical cyclogenesis in idealized numerical simulations. *J. Atmos. Sci.*, **73 (7)**, 2633–2642, doi:10.1175/jas-d-15-0380.1, URL http://dx.doi.org/10.1175/jas-d-15-0380.1.

Wing, A. A., and K. A. Emanuel, 2014: Physical mechanisms controlling self-aggregation of convection in idealized numerical modeling simulations. *J. Adv. Model. Earth Syst.*, **6 (1)**, 59–74, doi:10.1002/2013ms000269, URL http://dx.doi.org/10.1002/2013MS000269.

Yanai, M., 1961: A detailed analysis of typhoon formation. *J. Meteor. Soc. Japan*, **39 (4)**, 187–214.

Yu, J.-Y., C. Chou, and J. D. Neelin, 1998: Estimating the gross moist stability of the tropical atmosphere. *Journal of the Atmospheric Sciences*, **55 (8)**, 1354–1372, doi:10.1175/1520-0469(1998)055⟨1354:etgmso⟩2.0.co;2, URL https://doi.org/10.1175%2F1520-0469%281998%29055%3C1354%3Aetgmso%3E2.0.co%3B2.

Zhang, F., and K. Emanuel, 2016: On the role of surface fluxes and WISHE in tropical cyclone intensification. *J. Atmos. Sci.*, **73 (5)**, 2011–2019, doi:10.1175/jas-d-16-0011.1, URL http://dx.doi.org/10.1175/jas-d-16-0011.1.